JACS
JOURNAL OF THE AMERICAN CHEMICAL SOCIETY
Perspective
pubs.acs.org/JACS

Magnetically Responsive Nanostructures with Tunable Optical Properties

Mingsheng Wang and Yadong Yin*

Department of Chemistry, University of California, Riverside, California 92521, United States

ABSTRACT: Stimuli-responsive materials can sense specific environmental changes and adjust their physical properties in a predictable manner, making them highly desired components for designing novel sensors, intelligent systems, and adaptive structures. Magnetically responsive structures have unique advantages in applications, as external magnetic stimuli can be applied in a contactless manner and cause rapid and reversible responses. In this Perspective, we discuss our recent progress in the design and fabrication of nanostructured materials with various optical responses to externally applied magnetic fields. We demonstrate tuning of the optical properties by taking advantage of the magnetic fields' abilities to induce magnetic dipole−dipole interactions or control the orientation of the colloidal magnetic nanostructures. The design strategies are expected to be extendable to the fabrication of novel responsive materials with new optical effects and many other physical properties.

1. INTRODUCTION

Stimuli-responsive materials are of great interest recently due to their widespread potential applications.[1−3] They are capable of undergoing relatively large and rapid changes in their physical properties in response to small external stimuli, including but not limited to physical stimuli such as temperature,[4,5] light,[6,7] humidity,[8,9] mechanical stress,[10] and electric and magnetic fields[11−16] and chemical stimuli such as chemical interactions,[17,18] ionic strength, and pH.[19−23] Often, minute changes in the environment can trigger conformational changes in the responsive structures at the molecular or nanometer scale, resulting in changes of the overall physical or chemical properties of the bulk material.

Among various types of stimuli-response systems, magnetically responsive structures have attracted substantial research interest because they can respond instantaneously to external magnetic stimuli in a contactless manner, benefiting from the nature of magnetic interactions.[16,24,25] The magnetic-field-guided self-assembly of colloidal particles has long been considered as an important method for the fabrication of magnetically responsive structures.[26] Their advantages over other methods are obvious. The driving forces—magnetic dipole−dipole interactions between colloidal particles—can be efficiently induced by the application of an external magnetic field (created either by permanent magnets or electromagnets), allowing the quick assembly of particles within a second. The magnetic interactions are not sensitive to changes in experimental conditions, for example, the composition, temperature, ionic strength, and pH value of the solvents. More importantly, depending on the magnetic field directions and the orientation of induced magnetic dipoles in colloidal particles, it is convenient to control the magnetic interactions to be either attractive or repulsive. Therefore, by carefully programming the strength and spatial distribution of the magnetic field, the magnetic-field-guided assembly process can be precisely controlled, from the movement of a single nanosized object in a locally magnetized area to the globally synchronized motion of a large collection of objects.

In this Perspective, we highlight our recent advances in the design and fabrication of responsive structures via magnetic assembly of colloidal nanostructures. Instead of exhaustively going over all the responsive structures relevant to magnetic fields, we will focus on those with novel optical properties, including magnetically responsive photonic crystal structures, liquid crystals, and plasmonic structures. We will start by introducing general principles about magnetic interactions, and then discuss the basic design of colloidal building blocks as well as the methods for integrating magnetic assembly and control into the manipulation of optical properties. At the end, we will demonstrate magnetic tuning of the optical properties of the resultant superstructures and their potentials for various applications, such as optical modulators, displays, anti-counterfeiting devices, and sensors.

2. MAGNETIC RESPONSE OF NANOPARTICLES TO EXTERNAL MAGNETIC FIELDS

Colloidal particles experience various types of magnetic interactions in externally applied magnetic fields. Upon the application of the fields, colloidal particles are magnetized with an induced magnetic dipole moment $m = \chi HV$, where χ is the volume susceptibility of the particle, H is the local magnetic field, and V is the volume of the particle.[27] For a colloidal particle with a magnetic moment of m, its magnetic field H_1 sensed by an adjacent particle can be described by the following formula:

$$H_1 = [3(m\cdot r)r - m]/d^3$$

where r is the unit vector pointing from the center of the first particle to that of the second one, and d is the distance between the central points of these two particles. The dipole−dipole interaction energy of the second particle with the same magnetic moment m is then

$$U_2 = m\cdot H_1 = (3\cos^2\theta - 1)m^2/d^3$$

Received: March 3, 2016
Published: April 26, 2016

DOI: 10.1021/jacs.6b02346
J. Am. Chem. Soc. 2016, 138, 6315−6323

where θ is the angle between the field direction and the unit vector r. The dipole−dipole force exerted on the second particle by the first particle can be expressed as

$$F_{21} = \nabla(m \cdot H_1) = 3r(1 - 3\cos^2\theta)m^2/d^4$$

According to the above formulas, the dipole−dipole force is highly related to the configuration of the two dipoles. It is attractive when $0° \leq \theta < 54.09°$; repulsive in cases where $54.09° < \theta \leq 90°$; and zero at the critical angle of 54.09°. When the dipole−dipole force is strong enough to overcome thermal fluctuations, it drives the assembly of particles into one-dimensional (1D) chain-like structures to minimize their energy. For example, the dipole−dipole interaction energy between two ideal spherical magnetite particles with a diameter of 200 nm is estimated to be 4.47×10^{-18} J, when they are 10 μm apart. This value is much larger than their kinetic energy associated with Brownian motion: $E = {}^3/_2 kT = 6.21 \times 10^{-21}$ J, suggesting its dominance during the assembly process.

Practically, the magnetic fields for experimental uses are generated by a permanent magnet or an electromagnet, and are therefore not always homogeneous. Colloidal particles in an inhomogeneous magnetic field experience a force which drag them toward the direction of enhancing field strength.[28,29] The magnitude of this magnetophoretic force is monotonically related to the difference in the magnetic susceptibility between the colloidal particles and their surroundings. If the difference is larger enough, the magnetophoretic force can be approximated as $F_{phr} = \nabla B^2 \cdot V\chi/2\mu_0$, which is responsible for driving the movement of colloidal particles toward regions with the maximum field strength, and usually induces the creation of a gradient of particle concentration or eventually crystallization.

Magnetic shape anisotropy can also play a very important role in the magnetization of anisotropic colloidal particles.[30−32] A magnetized particle has induced magnetic poles at its surface, which produce a demagnetizing field in the opposing direction to the magnetization, $B_{demag} = -\mu_0 N \cdot M$, where N is the demagnetizing tensor, and m is the induced magnetic moment. Then the energy of the particle in its own demagnetizing field is given by the integral

$$E_{demag} = -\frac{1}{2}\int B_{demag} \cdot m \, dV = \frac{1}{2}\int \mu_0 (N \cdot m) \cdot m \, dV$$

For an infinitely long cylinder, the expression can be simplified as

$$E_{demag} = \frac{1}{4}\mu_0 m^2 \sin^2\theta$$

where θ is the angle between the major axis of the cylinder and the field direction. As a result, anisotropic colloidal particles spontaneously align their major axis parallel to the direction of external magnetic fields, in order to reduce the demagnetizing field as well as the energy associated with it. And for an infinitely expanded and/or very thin flat ellipsoid, the expression can be simplified as

$$E_{demag} = \frac{1}{2}\mu_0 m^2 \cos^2\theta$$

where θ is the angle between the normal plane of the thin flat ellipsoid and the field direction. As a result, an in-plane alignment of the magnetic moment of a thin ellipsoid is energetically favorable, and it spontaneously aligns its plane parallel to the direction of external magnetic fields, again for reducing the demagnetizing field and the associated energy.

3. MAGNETICALLY RESPONSIVE STRUCTURES FROM SPHERICAL NANOPARTICLES

Magnetic nanoparticles assemble into various kinds of structures under external magnetic fields, with key factors which determine the final assembly equilibrium being the magnitude of magnetic interactions as well as the local particle concentration. The strength of external magnetic fields directly determines both factors and enables full control of the assembly of nanoparticles into desired structures. On one hand, it determines the magnitude of induced magnetic dipole moments in particles and therefore controls the magnitude of dipole−dipole interactions between particles; on the other hand, the magnetophoretic force induced by the inhomogeneity of external magnetic fields drives the movement of particles and therefore creates gradient in the local particle concentration.

One of the most remarkable features of the assembly of magnetic nanoparticles is the formation of ordered structures. The transition from randomly distributed nanoparticles to 1D particle chains may represent the simplest switch between random and ordered states.[33−35] As a direct result of the directional magnetic dipole−dipole force, the chaining of nanoparticles occurs when the force is strong enough to overcome the thermal fluctuation. Structures of 1D particle chains formed by nanoparticles with various kinds of sizes and chemical compositions have been intensively investigated, with spherical superparamagnetic magnetite nanocrystal clusters chosen here as a model system for discussion.[36]

These superparamagnetic nanocrystal clusters are uniform colloidal spheres with average diameters in the range of 100−200 nm, and they are composed of tiny (<10 nm) magnetite (Fe_3O_4) nanocrystals (Figure 1a). They show acute magnetic

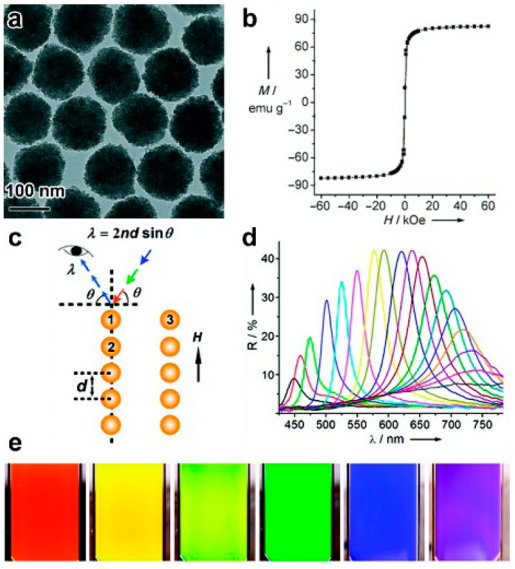

Figure 1. (a) Representative transmission electron microscopy image of the superparamagnetic nanocrystal clusters building blocks. (b) Magnetic hysteresis loop of the superparamagnetic nanocrystal clusters. (c) Scheme of Bragg diffraction from the 1D chain-like structures assembled from the building blocks. (d) Reflectance spectra of an aqueous dispersion of chain-like structures under magnetic fields with different strengths. (e) Digital photos of an aqueous dispersion of one typical nanocluster sample encapsulated in a capillary tube with a width of 1 cm under magnetic fields with increasing strengths from left to right. Reproduced with permission from ref 37. Copyright 2007 Wiley-VCH.

DOI: 10.1021/jacs.6b02346
J. Am. Chem. Soc. 2016, 138, 6315−6323

response and can be easily manipulated by external magnetic fields. Their zero net magnetic moments prevent them from magnetically induced permanent aggregation, and make the assembly process reversible. Meanwhile, their highly charged surfaces provide sufficient long-range interparticle electrostatic repulsion, which balances the magnetic dipole−dipole attraction and establish a force equilibrium within the chain-like structures, as schematically shown in Figure 1b. This equilibrium, however, is dynamic and sensitive to external fields. Slight changes in the field strengths can lead to destruction of the original equilibrium and reconstruction of a new equilibrium, and thus change the interparticle separation and the periodicities of chain-like structures.

When the magnetic particles are uniform in size and morphology, they assemble into chain-like 1D structures with regular separation, producing one of the smallest photonic structures with their diffraction wavelengths determined by the Bragg's law, $m\lambda = 2nd \sin\theta$, where n and d are their effective refractive index and periodicity, m the diffraction order, and θ the glancing angle of the incident light.[37,38] In response to the change of the strength of the external field, the periodicity of the chain-like structures alters. The diffraction wavelength is therefore responsive to external magnetic fields. After carefully optimizing the sizes of nanocrystal clusters, their diffraction wavelength or color can be effectively tuned within the visible light spectrum, from blue to green and to red, as shown in Figure 1d,e. The color change occurs instantly upon the change in field strength. Previous measurements suggested that the color switching frequency can reach ∼30 Hz under an alternating magnetic field.

In 1D chain-like structures, the magnetic dipole−dipole attractive forces are perfectly balanced by the electrostatic repulsive forces between particles. The interchain forces, mainly magnetic dipole−dipole repulsive forces, separate the chains away from each other. However, 1D chain-like structure is not the only phase of the self-assembly of spherical nanocrystal clusters. When a stronger magnetic field is applied, the magnetophoretic force induces the movement of particles toward regions with a higher field gradient. In addition, the interparticle dipole−dipole interaction becomes stronger. The 1D chain-like structures become less thermodynamically favorable under this condition and coalesce through a side-by-side assembly manner into zigzag multiple chains which further evolve into long-range 2D planar structures. Further increasing the particle concentration may lead to coalescence of the 2D planar structures and eventually produce 3D crystals (Figure 2).

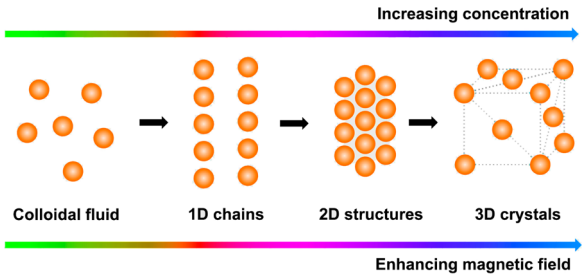

Figure 2. Schematic illustration showing the magnetically driven phase transition from colloidal fluid to 1D chain-like, 2D sheet-like, and 3D crystal structures. Reprinted with permission from ref 26. Copyright 2013 Elsevier.

The presence of 2D planar structures has been proposed and indirectly observed by a number of theoretical and experimental works, although a solid evidence for the existence of 2D planar structures has yet been achieved until a recent study.[39] By taking advantage of a sol−gel process, the dynamic 2D structures formed by the magnetite nanocrystal clusters can be stabilized for further characterization. Figure 3a shows the

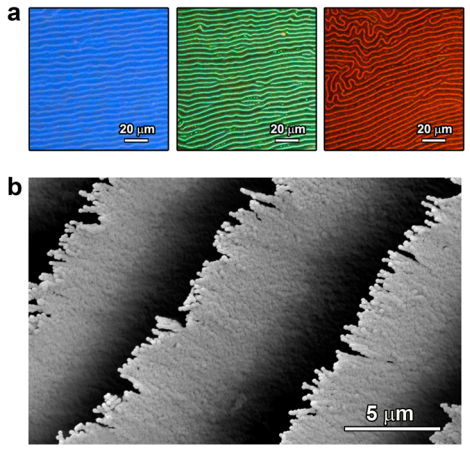

Figure 3. (a) Dark-field optical microscopy images of the top view of solidified 2D photonic planar structures with different diffraction colors. (b) Scanning electron microscopy image of the 2D planar structures viewed from the side. Reproduced with permission from ref 39. Copyright 2013 American Chemical Society.

dark-field optical microscopy images of the solidified 2D planar structures showing different photonic colors, as they were assembled from superparamagnetic nanocrystal clusters with different sizes. As they are vertically standing, they appear to be lines in a labyrinth pattern. Scanning electron microscopy (SEM) analysis, shown in Figure 3b, clearly reveals that these 2D structures are evolved from the side-by-side coalescence of 1D chain-like structures. They have well-defined sheet-like morphology, with width over tens of micrometers and length extendable beyond millimeter scale. The average thickness of the sheets is found to be less than 200 nm, which is equivalent to the diameter of a single magnetite nanocrystal cluster and is orders of magnitude smaller than the width and length of the sheets.

Further increasing the local particle concentration and the field strength may lead to the formation of highly crystalline 3D structures. As shown in Figure 4a−d, the average interparticle distance decreases in an enhancing field, resulting in blue shift of the diffraction wavelength of the 3D photonic structures. Small-angle X-ray scattering (SAXS) was used to investigate the 3D assembly process of the magnetite nanocrystal clusters.[40] In the absence of magnetic fields, the suspension of the nanocrystal clusters exhibits three major diffraction rings with q ratios of $\sqrt{8}:\sqrt{24}:\sqrt{32}$, which correspond to (220), (422), and (440) planes of a polycrystalline face-centered cubic (*fcc*) structure. The change in the structures is negligible in a 100 G magnetic field; however, reorganization of the polycrystalline *fcc* structure into a well-oriented single-crystalline-like structure occurs when the field strength further increases to 900 G, as evidenced by the evolution of diffraction patterns from rings to three sets of six diffraction spots (Figure 4e). These diffraction spots have q ratios of $\sqrt{3}:\sqrt{4}:\sqrt{7}$, which correspond to (110), (200), and (210) planes and suggest that magnetite nanocrystal

DOI: 10.1021/jacs.6b02346
J. Am. Chem. Soc. 2016, 138, 6315−6323

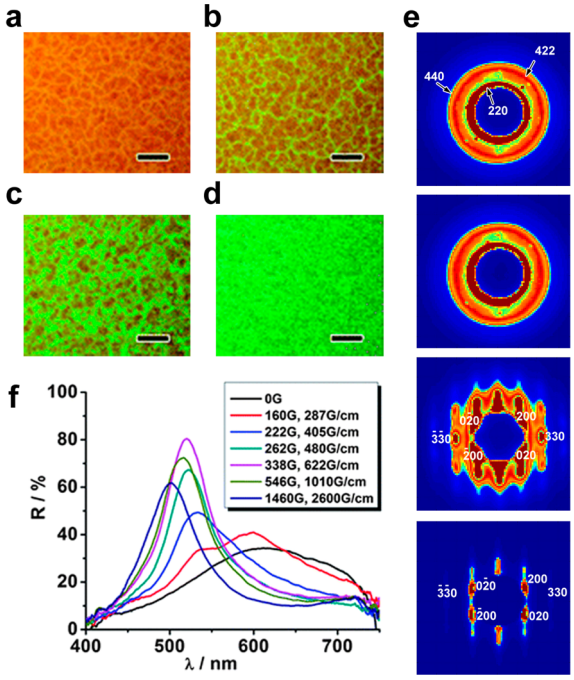

Figure 4. (a–d) Dark-field optical microscopy images of the crystalline 3D structures of nanocrystal clusters assembled in magnetic fields with strengths of (a) 0, (b) 120, (c) 200, and (d) 500 G. Scale bar: 20 μm. (e) SAXS pattern of 3D structures under different field strengths (from top to bottom: 0, 100, 900, and 1600 G). (f) Reflectance spectra of 3D structures under magnetic fields with varying strengths. Reproduced with permission from ref 40. Copyright 2012 Royal Society of Chemistry.

clusters formed a single-crystalline hexagonal-packed structures. Under an even stronger magnetic field (1600 G), the diffraction spots in the scattering pattern get further separated, indicating further improved crystallinity. The diffraction wavelengths of the 3D photonic structures also change during this process, with a blue shift from ~620 to ~500 nm (Figure 4f).

4. MAGNETICALLY RESPONSIVE STRUCTURES FROM ANISOTROPIC NANOPARTICLES

Self-assembly of nanoparticles into high-dimensional ordered structures usually requires a sufficiently high concentration; therefore, the average excluded volume of each particle becomes smaller, allowing less space for effective tuning of the collective property of the as-assembled superstructures. The use of anisotropic particles, however, is expected to bring more degrees of freedom for manipulation, as they often bear angular-dependent physical or chemical properties. Living systems, for example, Morpho butterfly, peacock, and *Chrysochroa fulgidissima*, often utilize periodical assemblies of anisotropic motifs such as plates and rods to produce their striking color effects.[41,42] Artificial colloidal assembly processes, however, are more or less limited to spherical, isotropic building blocks, mostly due to the challenges in making high-quality anisotropic building blocks and developing effective mechanisms for assembly.

In this context, rod-shaped magnetic nanoparticles are perhaps one of the best candidates for fabricating structures with angular- or orientation-dependent properties, as their orientation can be easily and instantly tuned by external magnetic fields. Recent efforts along this direction benefit from a unique two-step synthesis toward highly uniform and size-tunable anisotropic magnetic nanoparticles.[43] Nonmagnetic iron oxyhydroxide (FeOOH) nanorods with tunable sizes and aspect ratios were first prepared via the forced hydrolysis process of iron(III) chloride (Figure 5a). After being coated

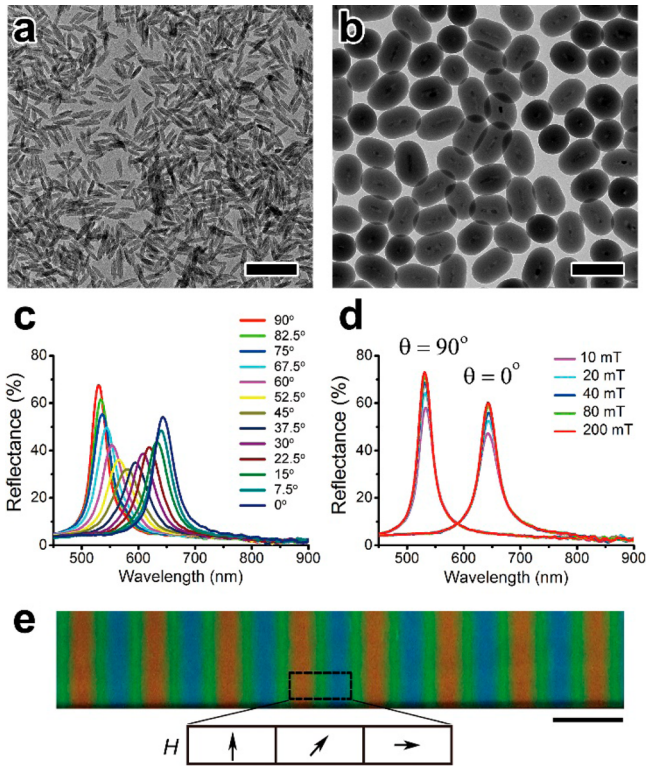

Figure 5. (a,b) TEM images of FeOOH nanorods and Fe@SiO_2 nanoellipsoids. Scale bar: 200 nm. (c) Reflectance spectra of the as-assembled structures from nanoellipsoids under magnetic fields with varying directions. (d) Reflectance spectra of as-assembled structures under magnetic fields with varying strengths. (e) Digital image of as-assembled photonic structures under a Halbach array with spatially rotating field directions (as described by the arrows), confirming their responsiveness to field directions. Scale bar: 5 mm. Reproduced with permission from ref 43. Copyright 2015 Wiley-VCH.

with a protection SiO_2 layer, they were reduced into magnetic substances, for example, magnetite or pure iron. The aspect ratio of final particles can be controlled by both the aspect ratio of initial FeOOH nanorods and the thickness of silica coating. The SiO_2 layer helps retain the anisotropic morphology of nanoparticles during the reduction process. More importantly, it acts as a physical barrier to separate the magnetic substances away from each other, and it provides an abundance of hydroxyl groups to enhance electrostatic repulsion between particles, which greatly enhances the dispersity of these anisotropic particles in various polar solvents and makes them excellent building blocks for the fabrication of magnetically responsive superstructures.

Similar to spherical particles, anisotropic particles can also serve as building blocks for the construction of 3D photonic structures. In the assembly of anisotropic building blocks, one should consider not only the positional order, as in the assembly of spherical building blocks, but also the orientational order. One unique consequence from this fact is that the photonic structures assembled from anisotropic particles often show strong angular dependence in their photonic response, as

DOI: 10.1021/jacs.6b02346
J. Am. Chem. Soc. 2016, 138, 6315–6323

demonstrated by a recent study in which elliptical Fe@SiO_2 core–shell particles were chosen.[43]

Figure 5b shows a typical sample of such Fe@SiO_2 particles which have a well-defined elliptical shape, with an average length of 190 nm and an average width of 130 nm. The orientation of elliptical nanoellipsoids can be easily controlled by external magnetic fields, owing to the embedded anisotropic magnetic cores. Upon application of a magnetic field, they simultaneously rotate and align themselves parallel to the field direction. When the direction of incident light is fixed, the rotation of nanoellipsoids is expected to result in changes in both the orientational orders and the translational orders of photonic assemblies. As indicated in Figure 5c, when the field direction is perpendicular to the incident light, the resultant photonic assemblies diffract light at a wavelength of ~520 nm. The diffraction peak gradually red-shifts as the field rotates toward the direction of incident light, and its wavelength reaches the maximum value of ~650 nm when the field direction is parallel to the incident light. The shift in diffraction wavelengths is fully reversible, and it happens instantly as the field direction changes.

In contrast to the field direction, the strength of external magnetic fields is found to have negligible effect on the diffraction wavelength. Instead, it plays an important role in perfecting the periodicity of photonic assemblies, as it determines to what degree the nanoellipsoids can be aligned. Owing to the limited amount of magnetic species embedded inside them, the alignment of nanoellipsoids requires a sufficiently strong magnetic field to allow the magnetic torque to overcome all the rotational resistance. As demonstrated in Figure 5d, the diffraction intensity of the photonic assemblies gradually increases with the field strength, suggesting a better orientational order of the building blocks within the assemblies. The use of elliptical particles as building blocks enables tuning the diffraction spectrum of 3D photonic structures simply by controlling the direction of external magnetic fields. The responsiveness to the magnetic field direction can be visually appreciated in Figure 5e, a digital image of photonic structures that were assembled from a dispersion of nanoellipsoids under a Halbach array with a spatially rotating magnetization pattern. More intriguingly, the dimensions and aspect ratios of elliptical particles can be easily tuned by the initial chemical synthesis, allowing the tuning range to effectively cover the entire visible spectrum.

Anisotropic particles with sufficiently large aspect ratios spontaneously gain orientational order as their concentration reaches a critical threshold, even in the absence of an external magnetic field. This process is analogous to the commonly discussed isotropic-to-nematic phase transition in organic lyotropic liquid crystals. The appearance of orientational order could be attributed to the reduced excluded volume of each anisotropic particle at increased volume fractions. The system sacrifices orientational entropy but gains translational entropy to reach an energetically more favorable nematic phase, in which most of the anisotropic particles align parallel.[44,45] Such nematic phase liquid crystals formed by anisotropic particles share a similar feature with commercial organic-molecules-based liquid crystals: the ability to change the direction of light polarization.

Generally, when a normal light transmits through a liquid crystal sandwiched between two cross polarizers, its intensity can be described as

$$I = I_0 \sin^2(2\alpha) \sin^2(\pi \Delta n L/\lambda)$$

where I_0 is the intensity of light transmitted through the first polarizer, α is the angle between the transmission axes of the polarizer and the long axis of the liquid crystal, Δn is the birefringence of the liquid crystal, L is the thickness of the sample, and λ is the wavelength of incident light.[46] One important advantage of using anisotropic magnetic nanoparticles to construct liquid crystals is that the resultant liquid crystals gain magnetic response, and their optical properties—polarization in this case—can be instantly and reversibly controlled by external magnetic fields (Figure 6a). In one

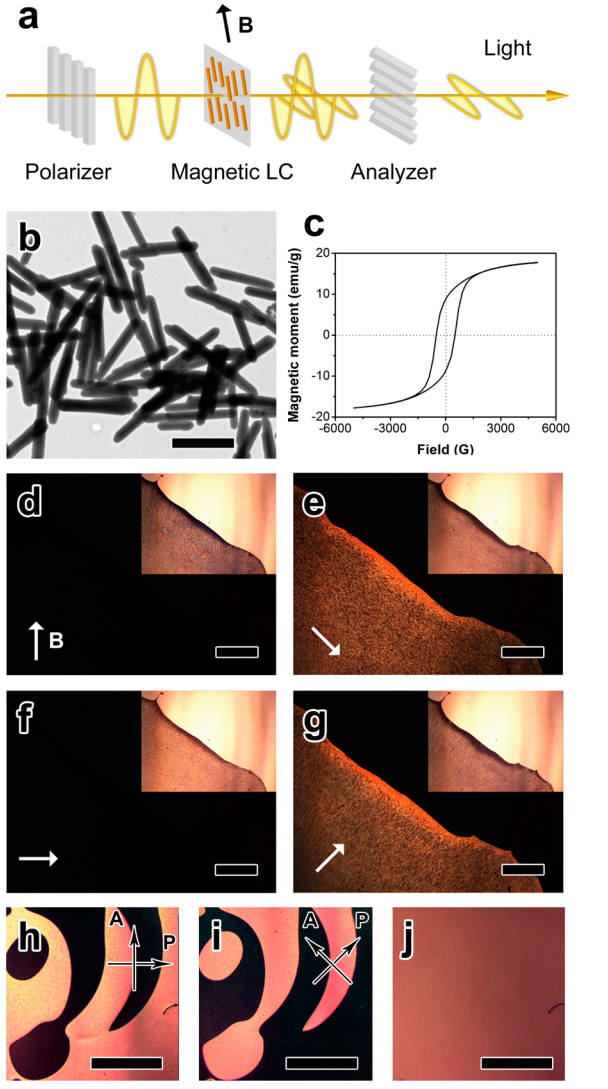

Figure 6. (a) Scheme of the basic working principle of magnetically actuated liquid crystals. (b) TEM image of the building blocks, Fe_3O_4@SiO_2 nanorods. Scale bar: 1 μm. (c) Magnetic hysteresis loop of Fe_3O_4@SiO_2 nanorods. (d–g) Polarized optical microscopy (POM) images of a liquid crystal sample under magnetic fields with different directions. The transmission axes of crossed polarizer are in the horizontal and vertical directions. The white arrow indicates the direction of magnetic fields. Inset: the corresponding bright-field OM images. (h,i) POM images of a liquid crystal film under crossed polarizers with different transmission axes. (j) OM images of the same liquid crystal film without any polarizer. Scale bar for d–j: 500 μm. Reproduced with permission from ref 47. Copyright 2014 American Chemical Society.

DOI: 10.1021/jacs.6b02346
J. Am. Chem. Soc. 2016, 138, 6315–6323

demonstration, long Fe_3O_4@SiO_2 nanorods (Figure 6b) were used as building blocks and were allowed to assemble into liquid crystals at a volume concentration of 10%.[47] Optical tuning of the as-formed liquid crystal by an external magnetic field was then investigated.

Owing to their ferromagnetic nature (Figure 6c), nanorods align their long axis parallel to the field direction instantly upon the application of an external magnetic field. As described by the above formula, when the field direction is parallel or perpendicular to the transmission axes of crossed polarizers, α equals to either 0° or 90°, and the total transmittance becomes zero, resulting in dark views in polarized optical microscopy (POM) (Figure 6d,f). When the field direction is turned 45°, the angle between the transmission axes of the polarizer and the long axis of the liquid crystal, α, changes to 45°. As a result, the total transmittance reaches the maximum, leading to bright views under POM (Figure 6e,g). In comparison, as suggested by the insets in Figure 6d–g, no significant change in the contrast of the same sample can be observed in the bright-field mode in response to the changes in the direction of the magnetic field.

Compared with molecular liquid crystals, another advantage of the nanorod-based liquid crystals is that the polarization states of the latter can be permanently fixed in a solid matrix. For example, by using a photocurable resin as a liquid medium, the nanorods could be first magnetically aligned, and then their orientation could be fixed by photocuring. With the aid of optical lithographic processes, it becomes convenient to produce thin patterned films with various optical polarizations, which show contrast in transmittance to a beam of linear polarized light. As demonstrated in Figure 6h, the areas where the orientation of the nanorods is parallel to the transmission axes of crossed polarizers are dark, while the areas where all nanorods are oriented 45° relative to crossed polarizers are bright, producing patterns with a clear contrast that is not observable under normal (nonpolarized) light (Figure 6j). When the orientation of the pattern changes relative to the transmission axes of the cross polarizers, the contrast of the pattern reverses, as shown in Figure 6i.

Magnetic alignment of anisotropic nanoparticles with external fields not only enables convenient control in the optical properties of their assemblies but also opens the door to the magnetic tuning of angular-dependent optical properties of other nonmagnetic anisotropic nanostructures.[48,49] Taking the plasmonic property of gold nanorods (AuNRs) as an example, AuNRs typically exhibit two plasmonic resonance modes: transverse mode and longitudinal mode.[50,51] The excitations of transverse and longitudinal modes are highly angular dependent, and are determined by the angle between the long axis of AuNRs and the electric field direction of the electromagnetic wave; in other words, the polarization of incident light. Generally, gold is diamagnetic, and AuNRs show negligible response to external magnetic fields; however, they can be made "artificially magnetic" by carefully attaching them to magnetic nanorods in a parallel manner.[52] Therefore, as magnetic nanorods align themselves to the direction of external magnetic fields, the attached AuNRs are aligned along the same direction, enabling an indirect magnetic control of their plasmonic excitation.

Figure 7a schematically illustrates three different configurations of plasmon excitations of AuNRs upon ordinary unpolarized light. For a beam of incident light along the y axis, both transverse and longitudinal plasmon modes of AuNRs can

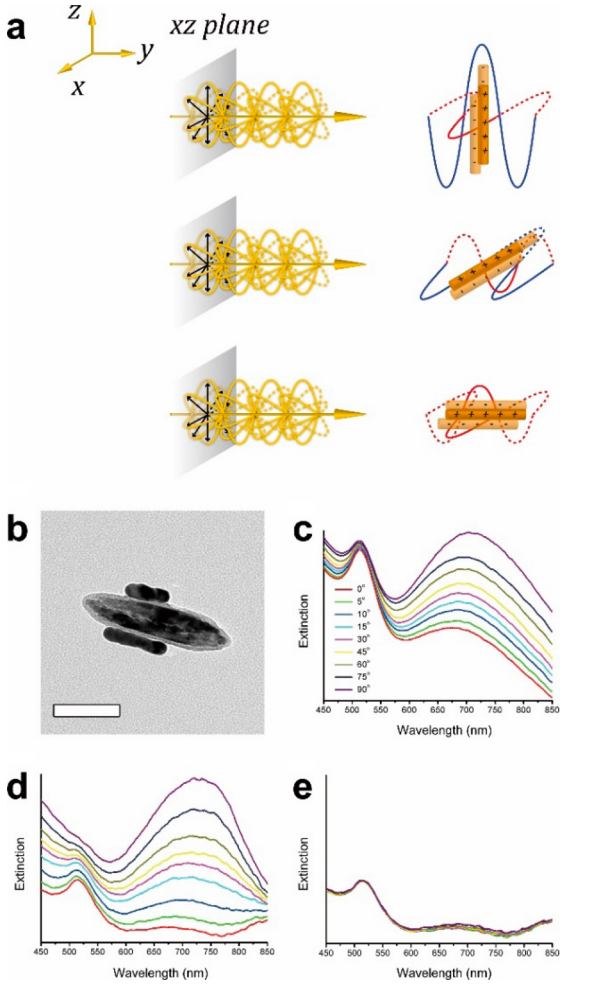

Figure 7. (a) Scheme for the magnetic tuning of AuNRs' plasmonic property. (b) Representative TEM image for the Au–magnetic nanorods hybrids. Scale bar: 100 nm. (c) Extinction spectra of nanorods hybrids under magnetic fields with different directions under nonpolarized light, with the angles represented for the difference between the field directions and the light propagation direction. (d,e) Extinction spectra of nanorods hybrids under z-polarized light, when magnetic fields are rotating in the yz plane and xy plane, respectively. Reproduced with permission from ref 52. Copyright 2013 American Chemical Society.

be excited when they are aligned along the x or z axis, perpendicular to the incident light. However, it is predicted that a significant difference will occur when AuNRs are aligned along the y axis, parallel to the incident light. As the electric field of light is always perpendicular to its propagation direction (y axis), the field direction is always parallel to the xz plane under this circumstance. As a result, the electron oscillation of AuNRs can only occur within the xz plane and is always parallel to their short axes, leading to the sole excitation of transverse plasmon.

The magnetic orientation control of AuNRs is achieved by attaching them to the surface of magnetic nanorods in a parallel manner. The surface of Fe_3O_4 nanorods is covered with a layer of silica, which is further functionalized with amino groups for linking to AuNRs. Owing to the high affinity between the gold surface and amino groups, AuNRs prefer to attach to the magnetic nanorods in a parallel manner by maximizing their contact areas, as evidenced by a representative transmission

DOI: 10.1021/jacs.6b02346
J. Am. Chem. Soc. 2016, 138, 6315–6323

electron microscopy (TEM) image of the resultant hybrid structures in Figure 7b.

The magnetic tuning of the plasmonic excitation has been confirmed by the extinction spectra in Figure 7c. When the angle between the direction of incident light and the external magnetic field decreases from 90° to 0°, the longitudinal plasmon mode decreases in magnitude, as suggested by the gradually attenuating peak at the wavelength of ∼700 nm. In the meantime, the magnitude of transverse plasmon mode changes only slightly, as indicated by the peak at ∼520 nm. More interestingly, when linearly polarized light is used as the light source, the selective excitation of the transverse or longitudinal mode can be achieved. In a simple demonstration, a beam of *z*-polarized light incident along the *y* axis. When AuNRs are aligned along the *z* axis by an external magnetic field, their spectrum shows a single strong peak at the longer wavelength, suggesting the maximum excitation of longitudinal plasmon mode and the extinction of transverse plasmon mode (Figure 7d). As they are rotating from *z* axis to *y* axis with external magnetic fields, the magnitude of their longitudinal plasmon mode decreases while the magnitude of their transverse plasmon mode increases. When the AuNRs are parallel to the incident light, the excitation of transverse plasmon mode reaches the maximum, as represented by the peak at ∼520 nm. The peak at ∼700 nm becomes ignorable, indicating good alignments of AuNRs along the magnetic field (along *y* axis). In contrast, magnetically rotating the AuNRs in the *xy* plane, from *x* axis to *y* axis does not significantly change the plasmonic property of AuNRs. Since *z* axis is perpendicular to the *xy* plane, only transverse plasmon mode of AuNRs can be excited under this circumstance (Figure 7e). Such optical switching mechanism is instantaneous, reversible, and can operate under considerably weak magnetic fields (several gauss) or even alternating magnetic fields with high frequency. The same strategy is expected to be extended to dynamic tuning of other anisotropic plasmonic nanostructures by magnetic fields.

5. CONCLUSION AND OUTLOOK

In this Perspective, we have presented the design strategies toward magnetically responsive structures with reversibly tunable optical properties. The overall design principle is to incorporate magnetic manipulation into nanostructured materials whose optical properties could be altered by their physical configuration, such as their assembly form and orientation. The key factors to the success of fabrications are the design of magnetically responsive building blocks with distinct sizes, shapes and chemical compositions, as well as the precise control over their interactions with each other and with the external fields. Based on these understandings, we have successfully synthesized various magnetic building blocks and demonstrated their assembly into field-responsive photonic crystal structures, liquid crystals, and plasmonic structures. Owing to the instantaneous nature of magnetic dipole−dipole interactions, they quickly respond to the change in the external magnetic fields, usually within less than one-tenth of a second, making them very promising candidates for a wide range of applications, such as color presentation and displays, anti-counterfeiting devices, novel optical components, and highly sensitive and selective chemical and biomedical sensors.

Despite the great progresses made in the development of magnetically responsive optical structures, there are still tremendous opportunities in this field. Many other optical effects could be controlled magnetically, for example, reflectance, transmittance, absorbance, scattering, interference, luminescence, and polarization including linear polarization and circular dichroism. We believe enabling effective magnetic control over these optical properties will provide many more novel functional materials that can help to address the grand challenges facing the modern society. For example, effective control over materials' transmittance by magnetic means may allow the fabrication of novel smart windows which can not only automatically adjust the lighting of a building but also regulate the heat transfer in and out of the house, significantly reduce the energy cost for lighting, heating, and air-conditioning. In another example, incorporating magnetic manipulation into luminescent materials may produce novel biosensors with magnetically switchable luminescent properties for highly sensitive detection of important biological events.

The key in the creation of novel magnetically responsive optical materials is the design and synthesis of building blocks that can incorporate magnetic manipulation into optical switching. In this regard, many new magnetic nanostructures could be used as the magnetic components to enable the active tuning. One example is the 2D planar magnetic nanostructures, such as nanodisks and nanoplates, which are expected to bring more degrees of freedom into the system design, new methods of tuning, as well as possible novel optical properties. The synthesis of such 2D magnetic nanostructures with uniform and controllable size distribution, however, requires additional research efforts. Other examples of novel magnetic components may include but not limit to materials with 3D morphologies including tetrahedral, cubic, octahedral, rhombohedral, and other shapes. These well-defined nanostructures have crystalline planes and axes along distinct orientations, which interact with light in different manners and thus add more complexity to the resultant superstructures.

Fundamental understandings to the self-assembly manner of the magnetic building blocks are also critical to the design and fabrication of resultant superstructures. Our current knowledge in this field, however, is limited. For instance, the 1D and 2D assembly of anisotropic building blocks have not been investigated in detail yet. Comprehensive phase diagrams for the self-assembly of nanoparticles under varying magnetic fields and different particle volume concentrations are highly desired. In addition, investigation of the assembly behavior of the magnetic building blocks under ultrastrong magnetic fields or high-frequency alternating magnetic fields are also of great interest, as it may help with the development of new magnetic tuning methods. Continued research in these directions is expected to provide better accuracy and precision in predicting and controlling the resultant structures. Advances in the synthesis of magnetic building blocks and the fundamental understandings about the magnetic-field-directed self-assembly manners are expected to prospect the fabrication of responsive structures with more complex design and more exciting and interesting optical effects.

A big challenge toward the practical applications of magnetically responsive structures is their scalability, from the synthesis of building blocks to their assembly to superstructures. In most chemistry laboratories, the synthesis of nanoparticles is typically in very small scale. For example, the typical synthesis scale of the superparamagnetic colloidal nanocrystal clusters discussed in this Perspective is around 30 mg and that of the anisotropic nanorods ranging from milligram scale to gram scale. However, most industrial applications require materials at the kilogram or even ton

DOI: 10.1021/jacs.6b02346
J. Am. Chem. Soc. 2016, 138, 6315−6323

scale, which are more than 6 orders of magnitude larger in the quantity. The scale-up synthesis of nanoparticles requires a much more sophisticated control on the reaction process and usually specially designed reaction apparatus. Many effects such as temperature gradient, concentration gradient, and heating rate which could be negligible in small-scale synthesis may become crucial for synthesis at large scales. It is feasible to scale up the synthesis for over 10 times in a chemistry laboratory by fine-tuning the reactions conditions; however, synthesis at further increased scales would require redesign of the reaction setups by considering the much altered materials and heat transport. On the other hand, as the amount of building blocks increases, more factors need to be considered during their assembly into the responsive superstructures, which include but not limit to the concentration gradients in the particle dispersions and the homogeneity of magnetic fields, as well as the time cost.

Although in this Perspective we focused our discussions on only the magnetic tuning of optical properties, the design strategies can be easily extended to the fabrication of responsive materials with other magnetically tunable physical properties, such as shape, porosity, fluidity, and mechanical and electrical properties. We are confident that further development in this multidisciplinary field will produce a wide range of smart materials with their physical properties magnetically tunable in a wide range of scales, and will further provide enormous opportunities for the creation of novel intelligent systems, sensors and actuators, and adaptive structures that are needed for digitalizing the modern society.

AUTHOR INFORMATION

Corresponding Author

*yadong.yin@ucr.edu

Notes

The authors declare no competing financial interest.

ACKNOWLEDGMENTS

The research discussed in this Perspective has been supported at different stages by the U.S. National Science Foundation (DMR-0956081, CHE-1308587) and U.S. Army Research Laboratory (W911NF-10-1-0484). Y.Y. also thanks the Research Corporation for Science Advancement for the Cottrell Scholar Award and DuPont for the Young Professor Grant.

REFERENCES

(1) Stuart, M. A. C.; Huck, W. T. S.; Genzer, J.; Muller, M.; Ober, C.; Stamm, M.; Sukhorukov, G. B.; Szleifer, I.; Tsukruk, V. V.; Urban, M.; Winnik, F.; Zauscher, S.; Luzinov, I.; Minko, S. *Nat. Mater.* **2010**, *9*, 101.

(2) Holtz, J. H.; Asher, S. A. *Nature* **1997**, *389*, 829.

(3) Alarcon, C. D. H.; Pennadam, S.; Alexander, C. *Chem. Soc. Rev.* **2005**, *34*, 276.

(4) Moon, H. J.; Ko, D. Y.; Park, M. H.; Joo, M. K.; Jeong, B. *Chem. Soc. Rev.* **2012**, *41*, 4860.

(5) Liu, W. G.; Zhang, B. Q.; Lu, W. W.; Li, X. W.; Zhu, D. W.; De Yao, K.; Wang, Q.; Zhao, C. R.; Wang, C. D. *Biomaterials* **2004**, *25*, 3005.

(6) Schumers, J. M.; Fustin, C. A.; Gohy, J. F. *Macromol. Rapid Commun.* **2010**, *31*, 1588.

(7) Alvarez-Lorenzo, C.; Bromberg, L.; Concheiro, A. *Photochem. Photobiol.* **2009**, *85*, 848.

(8) Sidorenko, A.; Krupenkin, T.; Taylor, A.; Fratzl, P.; Aizenberg, J. *Science* **2007**, *315*, 487.

(9) Ge, J. P.; Goebl, J.; He, L.; Lu, Z. D.; Yin, Y. D. *Adv. Mater.* **2009**, *21*, 4259.

(10) Arsenault, A. C.; Clark, T. J.; Von Freymann, G.; Cademartiri, L.; Sapienza, R.; Bertolotti, J.; Vekris, E.; Wong, S.; Kitaev, V.; Manners, I.; Wang, R. Z.; John, S.; Wiersma, D.; Ozin, G. A. *Nat. Mater.* **2006**, *5*, 179.

(11) Kim, S. Y.; Lee, Y. M. *J. Appl. Polym. Sci.* **1999**, *74*, 1752.

(12) Ge, J.; Neofytou, E.; Cahill, T. J.; Beygui, R. E.; Zare, R. N. *ACS Nano* **2012**, *6*, 227.

(13) Li, H.; Yuan, Z.; Lam, K. Y.; Lee, H. P.; Chen, J.; Hanes, J.; Fu, J. *Biosens. Bioelectron.* **2004**, *19*, 1097.

(14) Medeiros, S. F.; Santos, A. M.; Fessi, H.; Elaissari, A. *Int. J. Pharm.* **2011**, *403*, 139.

(15) Filipcsei, G.; Csetneki, I.; Szilagyi, A.; Zrinyi, M. *Adv. Polym. Sci.* **2007**, *206*, 137.

(16) He, L.; Wang, M. S.; Ge, J. P.; Yin, Y. D. *Acc. Chem. Res.* **2012**, *45*, 1431.

(17) Yan, X. Z.; Wang, F.; Zheng, B.; Huang, F. H. *Chem. Soc. Rev.* **2012**, *41*, 6042.

(18) Popat, A.; Ross, B. P.; Liu, J.; Jambhrunkar, S.; Kleitz, F.; Qiao, S. Z. *Angew. Chem. Int. Ed.* **2012**, *51*, 12486.

(19) Zhao, B.; Moore, J. S. *Langmuir* **2001**, *17*, 4758.

(20) Markland, P.; Zhang, Y. H.; Amidon, G. L.; Yang, V. C. *J. Biomed. Mater. Res.* **1999**, *47*, 595.

(21) Solomatin, S. V.; Bronich, T. K.; Bargar, T. W.; Eisenberg, A.; Kabanov, V. A.; Kabanov, A. V. *Langmuir* **2003**, *19*, 8069.

(22) Carrick, L. M.; Aggeli, A.; Boden, N.; Fisher, J.; Ingham, E.; Waigh, T. A. *Tetrahedron* **2007**, *63*, 7457.

(23) Zhang, K. P.; Luo, Y. L.; Li, Z. Q. *Soft Mater.* **2007**, *5*, 183.

(24) Ge, J. P.; Yin, Y. D. *J. Mater. Chem.* **2008**, *18*, 5041.

(25) Ge, J. P.; He, L.; Hu, Y. X.; Yin, Y. D. *Nanoscale* **2011**, *3*, 177.

(26) Wang, M. S.; He, L.; Yin, Y. D. *Mater. Today* **2013**, *16*, 110.

(27) Griffiths, D. J. *Introduction to electrodynamics*, 3rd ed.; Prentice Hall: Upper Saddle River, NJ, 1999.

(28) Benelmekki, M.; Martinez, L. M.; Andreu, J. S.; Camacho, J.; Faraudo, J. *Soft Matter* **2012**, *8*, 6039.

(29) Lim, J.; Lanni, C.; Evarts, E. R.; Lanni, F.; Tilton, R. D.; Majetich, S. A. *ACS Nano* **2011**, *5*, 217.

(30) Vokoun, D.; Beleggia, M.; Heller, L.; Sittner, P. *J. Magn. Magn. Mater.* **2009**, *321*, 3758.

(31) Fuller, H. W.; Sullivan, D. L. *J. Appl. Phys.* **1962**, *33*, 1063.

(32) Joseph, R. I.; Schlomann, E. *J. Appl. Phys.* **1961**, *32*, 1001.

(33) Hu, Y. X.; He, L.; Yin, Y. D. *Angew. Chem. Int. Ed.* **2011**, *50*, 3747.

(34) Guo, L.; Liang, F.; Wen, X. G.; Yang, S. H.; He, L.; Zheng, W. Z.; Chen, C. P.; Zhong, Q. P. *Adv. Funct. Mater.* **2007**, *17*, 425.

(35) Zhang, Y.; Sun, L.; Fu, Y.; Huang, Z. C.; Bai, X. J.; Zhai, Y.; Du, J.; Zhai, H. R. *J. Phys. Chem. C* **2009**, *113*, 8152.

(36) Ge, J. P.; Hu, Y. X.; Biasini, M.; Beyermann, W. P.; Yin, Y. D. *Angew. Chem. Int. Ed.* **2007**, *46*, 4342.

(37) Ge, J. P.; Hu, Y. X.; Yin, Y. D. *Angew. Chem. Int. Ed.* **2007**, *46*, 7428.

(38) Ge, J. P.; Yin, Y. D. *Adv. Mater.* **2008**, *20*, 3485.

(39) Zhang, Q.; Janner, M.; He, L.; Wang, M. S.; Hu, Y. X.; Lu, Y.; Yin, Y. D. *Nano Lett.* **2013**, *13*, 1770.

(40) He, L.; Malik, V.; Wang, M. S.; Hu, Y. X.; Anson, F. E.; Yin, Y. D. *Nanoscale* **2012**, *4*, 4438.

(41) Ingram, A. L.; Parker, A. R. *Philos. Trans. R. Soc., B* **2008**, *363*, 2465.

(42) Galusha, J. W.; Richey, L. R.; Jorgensen, M. R.; Gardner, J. S.; Bartl, M. H. *J. Mater. Chem.* **2010**, *20*, 1277.

(43) Wang, M. S.; He, L.; Xu, W. J.; Wang, X.; Yin, Y. D. *Angew. Chem. Int. Ed.* **2015**, *54*, 7077.

(44) Onsager, L. *Ann. N. Y. Acad. Sci.* **1949**, *51*, 627.

(45) Vroege, G. J.; Lekkerkerker, H. N. W. *Rep. Prog. Phys.* **1992**, *55*, 1241.

(46) Collings, P. J.; Hird, M. *Introduction to liquid crystals chemistry and physics*; Taylor & Francis: London, 1997.

DOI: 10.1021/jacs.6b02346
J. Am. Chem. Soc. 2016, 138, 6315−6323

(47) Wang, M. S.; He, L.; Zorba, S.; Yin, Y. D. *Nano Lett.* **2014**, *14*, 3966.
(48) Erb, R. M.; Libanori, R.; Rothfuchs, N.; Studart, A. R. *Science* **2012**, *335*, 199.
(49) Bubenhofer, S. B.; Athanassiou, E. K.; Grass, R. N.; Koehler, F. M.; Rossier, M.; Stark, W. J. *Nanotechnology* **2009**, *20*, 485302.
(50) Chen, H. J.; Shao, L.; Li, Q.; Wang, J. F. *Chem. Soc. Rev.* **2013**, *42*, 2679.
(51) Link, S.; El-Sayed, M. A. *J. Phys. Chem. B* **1999**, *103*, 8410.
(52) Wang, M. S.; Gao, C. B.; He, L.; Lu, Q. P.; Zhang, J. Z.; Tang, C.; Zorba, S.; Yin, Y. D. *J. Am. Chem. Soc.* **2013**, *135*, 15302.

DOI: 10.1021/jacs.6b02346
J. Am. Chem. Soc. 2016, 138, 6315−6323